

Calculating the Lyapunov exponents of a piecewise-smooth soft impacting system with a time-delayed feedback controller

Zhi Zhang, Yang Liu*, Jan Sieber

^a*College of Engineering Mathematics and Physical Sciences, University of Exeter, Harrison Building, North Park Road, Exeter EX4 4QF, UK*

Abstract

Lyapunov exponent is a widely used tool for studying dynamical systems. When calculating Lyapunov exponents for piecewise-smooth systems with time-delayed arguments one faces the variational problem of lack of continuity. This paper studies how to build a variational equation for the efficient construction of Jacobian along trajectories of the delayed nonsmooth system. Trajectories of the piecewise-smooth system may encounter the so-called grazing event at where the trajectory approaches discontinuity surface in the state space in a non-transversal manner. For this event we develop a grazing point estimation algorithm to ensure the accuracy of trajectories for the nonlinear and the variational equations. We show that the eigenvalues of the Jacobian matrix computed by the algorithm converge with an order consistent with the order of the numerical integration method, therefore guaranteeing the reliability of our proposed numerical method. Finally, the method is validated on a periodically forced impacting oscillator under the time-delayed feedback control.

Keywords: Lyapunov exponents; Piecewise-smooth dynamical system; Delay differential equation; Grazing; Impact oscillator.

1. Introduction

Analysing grazing bifurcation for nonsmooth systems is a challenging task [1]. In general, for vibro-impact systems, such as ship mooring interactions [2], bearing looseness [3] and the multi-degree-of-freedom impact oscillators [4], they may have abundant coexisting attractors when grazing occurs, and any tiny differences in modelling will lead to different motion of the system [5, 6]. For example, the motion of an impact oscillator experiences significantly change due to a slight variation on its parameter when grazing bifurcation is encountered [7]. In [8], Nordmark studied the characteristic scaling behaviour in grazing bifurcation, and used the self-similarity under scaling to derive a renormalised mapping. Nordmark [9] presented the grazing bifurcation of a hard impact oscillator which had singular Jacobian of Poincaré map by using the first-order Taylor expansion. It has shown that the more accurate grazing bifurcation to be depicted, the more precise the stability of the oscillator to be studied. This paper will study a new method to improve the accuracy of calculation of grazing bifurcation by estimating the impacting moment. Based on this accurate grazing trajectory, stability analysis of the system can be carried out.

In many applications [10–14], delay is always considered in their differential equations in which the derivative of the unknown functions at a certain time depends on the value of the function at previous

Email addresses: zz326@exeter.ac.uk (Zhi Zhang), y.liu2@exeter.ac.uk (Yang Liu*), j.sieber@exeter.ac.uk (Jan Sieber)

time, the so-called delay differential equations (DDEs). For example, Zhang *et al.* [12] studied a delayed pest control model which was a high-dimensional differential equation with impulsive effects at different fixed impulsive moments. In [13], Carvalho and Pinto used a mathematical model with delay to describe the dynamics of AIDS- related cancers with the treatment of HIV and chemotherapy. In [14], Yan *et al.* used the basin of a time-delayed system modelling cutting process to determine the unsafe cutting zone. The above studies concern about smooth DDEs. The analysis of nonsmooth DDEs is more challenging due to the lack of an accurate algorithm for computing the grazing events. Until now, there are very few systematic studies regarding to nonsmooth DDEs, which is the focus of this paper. The present work will study a new algorithm to determine the occurrence of grazing for improving computational accuracy and a new method for calculating Lyapunov exponents (LEs) along the trajectories of a nonsmooth DDE.

LE is an important tool for studying the stability of dynamical system. If the largest LE is greater than zero, any small perturbation on initial condition will result in an exponential divergence of the resulting perturbed trajectory until the distance between the perturbed and unperturbed trajectories is no longer small. This sensitivity with respect to initial condition is one of the defining features of chaos. Therefore, the development of an efficient method for calculating the LEs of dynamical system is an active area of research, see e.g. [15–22]. On the one hand, Benettin *et al.* [16] introduced a systematic method for estimating the LEs of smooth dynamical systems. Wolf *et al.* [17] developed a method for extracting the largest LE from an experimental time series. For nonsmooth systems, Müller [20] developed a model-based algorithm to calculate the LEs of the nonlinear dynamical systems with discontinuities. As a result, the required linearised equations must be supplemented by certain transition conditions at the instants of discontinuities. In [21], Dellago *et al.* generalised Benettin’s classical algorithm and applied it to the case of dynamical systems where smooth streaming was interrupted by a differentiable map at discrete times. Lamba and Budd [23] has shown that the largest LE has a discontinuous jump at grazing bifurcation in Filippov systems and scales like $1/|\ln \epsilon|$, where ϵ is the bifurcation parameter. On the other hand, since DDE is an infinite dimensional system, calculation of LEs for nonsmooth DDEs is more complicated than the smooth one. In principle, DDEs could be approximated by ordinary differential equations (ODEs) which can be linearised by numerical integration [24, 25], so Poincaré map can be constructed for calculating LEs. Studies by Repin [26] and Györi and Turi [27] have shown that DDEs can be analysed using approximating high-dimensional ODEs. However, if delay time is large, calculating the LEs of nonsmooth DDEs needs to store excessive history data points during delay period compared to smooth DDEs [28–30], e.g. the data at the discontinuous moments. In this case the global convergence of the system cannot be guaranteed. Therefore, it may cause inaccuracy in calculating the eigenvalues of Jacobian matrix which is used for estimating the LEs of nonsmooth DDEs.

The contribution of the present work is the development of a novel method for precisely calculating the LEs of piecewise-smooth differential equations with a delay argument, which can provide an improved accuracy in stability analysis for periodic orbits. If an algorithm cannot estimate the point of discontinuity along trajectory with an accuracy of the same order as its integration method, especially in the grazing event, the expected discontinuous coefficients of the variational problem will have unexpectedly low accuracy leading to an accumulation of errors. Similar work was reported by Müller [20] who studied a method for constructing the map of nonsmooth systems with discontinuity, and combined it with the map obtained from continuous process to generate an integrated Jacobian matrix for calculating LEs. However, Müller’s approach is difficult to be implemented for piecewise-smooth DDE due to its high dimension and complex dynamics, which could cause a high computational cost and an accumulation of computational errors at discontinuous moments. In order to address this issue, Poincaré map that consists of many small

local maps at each time step will be constructed in the present work for linearising the delayed piecewise-smooth oscillator. Since Poincaré map requires accurate information of the discontinuous moment when impact occurs, a grazing estimation algorithm will be introduced, and therefore, an accurate Jacobian matrix of the oscillator can be obtained. The novelty of our proposed method is that it can estimate the point of discontinuity locally along trajectories of piecewise-smooth DDEs, improving the accuracy of computations of system trajectory and LEs. The proposed method can also be extended to other nonsmooth dynamical systems, such as the hard impact oscillator with a time-delayed controller or stick-slip vibrations with a delay term. To demonstrate the reliability of the method, we will carry out an error analysis for the nonzero eigenvalues of the Jacobian by adopting the spectral approximation methods introduced by Chatelin [31] and Breda *et al.* [28, 30]. Our study indicates that the proposed method can reduce error for the nonzero eigenvalues of the Jacobian by increasing the dimensions of the approximated system (ODEs) slightly, which can be generated from linearising the DDEs by numerical integration.

The rest of this paper is organised as follows. Section 2 introduces the mathematical model of the periodically forced mechanical oscillator subjected to a one-sided soft impact. This is followed by some basic relevant definitions and preparations. Section 3 presents the method for constructing the Jacobian of Poincaré map of piecewise-smooth DDEs. However, such a construction is inaccurate due to the nonsmoothness of the considered system. Thus, Section 4 studies the estimation method for determining the points of discontinuity accurately. Here, two cases of grazing events are considered based on the geometry of the trajectory. Section 5 uses the linear operator theory to carry out an error analysis for the eigenvalues of the Jacobian, which can validate the reliability of our proposed method. In Section 6, the steps for computing LEs are detailed. Examples and several control scenarios of the oscillator are presented in Section 7 to demonstrate the accuracy of the method. Finally, some concluding remarks are drawn in Section 8.

2. Mathematical model and relevant preparations

The impact oscillator shown in Fig. 2.1 represents a mechanical system encountering intermittent so-called soft impacts, which will be studied in the present work. The nondimensional equations of motion of the impact oscillator can be written in a compact form as follows [7, 32]:

$$\begin{cases} x'(\tau) = v(\tau), \\ v'(\tau) = a\omega^2 \sin(\omega\tau) - 2\zeta v(\tau) - x(\tau) - \beta(x(\tau) - e)H(x(\tau) - e), \end{cases} \quad (2.1)$$

where $H(\cdot)$ stands for the Heaviside step function and x' , v' denote differentiation with respect to the nondimensional time τ . The discontinuity boundary is fixed at $x = e$, with $e > 0$ being the nondimensional gap to the rest point of the linear spring. Eq. (2.1) was nondimensionalised from the representation in Fig. 2.1 by introducing the following variables and parameters

$$\begin{aligned} \omega_n &= \sqrt{\frac{k_1}{m}}, & \tau &= \omega_n t, & \omega &= \frac{\Omega}{\omega_n}, & \zeta &= \frac{c}{2m\omega_n}, \\ x &= \frac{y}{y_0}, & e &= \frac{g}{y_0}, & a &= \frac{A}{y_0}, & \beta &= \frac{k_2}{k_1}, \end{aligned}$$

where $y_0 > 0$ is an arbitrary reference distance, ω_n is the natural angular frequency, ω is the frequency ratio, β is the stiffness ratio, ζ is the damping ratio, and a is the nondimensionalized forcing amplitude.

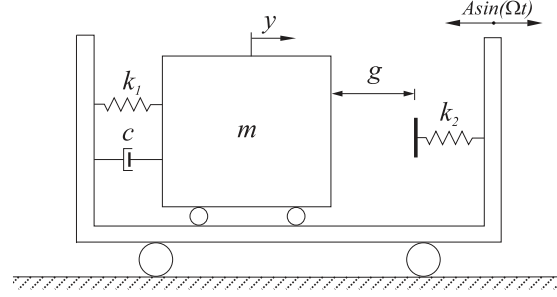


Figure 2.1: Physical model of the soft impact oscillator [32].

In the present work, we will consider a control signal $u(\tau)$, $\tau \geq 0$, which will be superimposed on the system's external excitation as follows

$$\begin{cases} x'(\tau) = v(\tau), \\ v'(\tau) = (a\omega^2 \sin(\omega\tau) + u(\tau)) - 2\zeta v(\tau) - x(\tau) - \beta(x(\tau) - e)H(x(\tau) - e), \end{cases} \quad (2.2)$$

where

$$u(\tau) = k(v(\tau - \tau_d) - v(\tau)), \quad \tau \geq 0, \quad (2.3)$$

defines the proportional feedback controller that feedbacks the difference between the current measurement of v and a measurement of v from some time τ_d ago [33]. In the expression above, $k \geq 0$ represents the feedback gain of the controller and $\tau_d > 0$ stands for a predefined time delay.

Eq. (2.2) can be rewritten in the form of a general piecewise continuous DDE with a periodic external excitation as

$$\begin{cases} \dot{y}(t) = f_1(y(t), y(t - \tau_d)) + p(t), & \text{for } H(y(t), e) > 0, \\ \dot{y}(t) = f_2(y(t), y(t - \tau_d)) + p(t), & \text{for } H(y(t), e) < 0, \\ y(t^+) = y(t^-), & \text{for } H(y(t), e) = 0, \end{cases} \quad (2.4)$$

where $f_{1,2} : \mathbb{R}^d \times \mathbb{R}^d \rightarrow \mathbb{R}^d$, $H : \mathbb{R}^d \rightarrow \mathbb{R}$ is sufficiently smooth function and $p : \mathbb{R}^+ \rightarrow \mathbb{R}^d$ is smooth and periodic with the period $T > 0$ and $\tau_d > 0$. In the present work, we only consider one single delay in the system for simplicity, and assume that for any $y, \bar{y}, y_d, \bar{y}_d \in \mathbb{R}^d$, it satisfies

$$|f_{1,2}(y, y_d) - f_{1,2}(\bar{y}, \bar{y}_d)| \leq l_1|y - \bar{y}| + l_2|y_d - \bar{y}_d|,$$

where $y_d = y(t - \tau_d)$ and $l_1, l_2 \geq 0$, and for any $y, \bar{y} \in \mathbb{R}^d$, it has $|H(y, e) - H(\bar{y}, e)| \leq l_3|y - \bar{y}|$, where $l_3 \geq 0$ and $|\cdot|$ is a given norm on \mathbb{R}^d . We assume that the initial condition is from a suitable initial function on $[t_0, t_0 - \tau_d]$. The general form (2.4) belongs to the class of *hybrid dynamical systems* [1], which consists of a flow (in our case only forward in time), combined with discrete events.

Take $N \in \mathbb{Z}^+$ sufficiently large, and define the grid points $\tau_d^i := i\frac{\tau_d}{N}$, $i = 0, \dots, N$, and $u_i(t) := y(t - \tau_d^i)$ for all $t \geq 0$, $i = 0, \dots, N$, Eq. (2.4) can be approximated by the $d(N + 1)$ dimensional piecewise-smooth abstract Cauchy problem studied in [26], which will be presented in Section 3. This approximation method has also been studied by Krasovskii [34], and particularly, the solution of the approximated system uniformly converges to its original DDEs when $N \rightarrow \infty$. By using the same approach, Györi and Turi [27] and Banks [35] carried out convergence analyses for two DDEs. Breda *et al.* [29] studied the characteristic roots of DDEs, and used Runge-Kutta method to construct a high-dimensional approximating system.

The nonzero eigenvalues of evolution operators were computed through a pseudospectral collection, which were used to analyse the asymptotic stability of DDEs. Since Eq. (2.4) is a piecewise-smooth DDE whose trajectories can encounter discontinuities intermittently, the methods used for smooth DDEs are not available. Therefore, motivated by the periodic forcing of Eq. (2.4), our plan here is to derive a Poincaré map for discretising the system and study its stability by considering the Jacobian matrix of the map. After such a reduction to the Poincaré map, we will be able to define LEs for this time-discrete map.

For the piecewise DDE (2.4), we consider a constant phase surface as the Poincaré section defined by $P_s^T := \{(y, t) \in \mathbb{R}^d \times \mathbb{R}^+ \mid t = t_0 + kT, k \in \mathbb{Z}^+\}$, and the relevant Poincaré map can be written as

$$P : P_s^T \rightarrow P_s^T. \quad (2.5)$$

Then the LEs of the Poincaré map (2.5) can be introduced as follows.

Definition 2.1. [15] For any initial condition x_0 , let $\{x_m\}_{m=0}^\infty$ be the corresponding orbit of a n -dimensional discrete-time system P , and let $\lambda_0^m, \dots, \lambda_n^m$ be the eigenvalues of $DP^m(x_0)$, the Lyapunov numbers of x_0 are

$$\vartheta_i := \lim_{m \rightarrow \infty} |\lambda_i^m|^{\frac{1}{m}}, i = 0, \dots, n, \quad (2.6)$$

whenever the limit exists.

3. Constructing the Jacobian matrix of the Poincaré map

For the nonsmooth system with a delay τ_d smaller than its forcing period T , i.e. $0 < \tau_d < T$, the period T can be written as $T = n\tau_d + \Delta t$, for $n \in \mathbb{Z}^+$ and $\Delta t \in [0, \tau_d)$. For any time interval $[t_m, t_m + \tau_d]$, where $t_m = t_1 + (m-1)T$, $t_1 = t_0$ and $m \in \mathbb{Z}^+$, the solution of system (2.4) can be approximated by N samples at the step $h = \frac{\tau_d}{N}$ by using numerical integration. By using the modified Euler integration [36], it gives

$$\begin{aligned} u_0(t_m + h) = & u_0(t_m) + \frac{h}{2} [f_j(u_0(t_m), u_0(t_m - hN)) \\ & + f_j(u_0(t_m + h), u_0(t_m - h(N-1)))] + \frac{h}{2} [p(t_m) + p(t_m + h)], \end{aligned} \quad (3.1)$$

where

$$\begin{cases} j = 1, & \text{if } H(u_0(t_m), e) > 0, \\ j = 2, & \text{if } H(u_0(t_m), e) < 0, \\ u_0(t_m^+) = u_0(t_m^-), & \text{if } H(u_0(t_m), e) = 0. \end{cases}$$

After $N + 1$ iterations, a local map for the delayed time interval $[t_m, t_m + \tau_d]$ can be defined as $P_d : \mathbb{R}^{d(N+1)} \rightarrow \mathbb{R}^{d(N+1)}$, which satisfies

$$U_{m,1} = P_d(U_{m,0}), \quad (3.2)$$

where $U_{m,0} := (u_N^T(t_m), \dots, u_1^T(t_m), u_0^T(t_m))^T \in \mathbb{R}^{d(N+1)}$ and $U_{m,1} := (u_N^T(t_m + \tau_d), \dots, u_1^T(t_m + \tau_d), u_0^T(t_m + \tau_d))^T \in \mathbb{R}^{d(N+1)}$. Repeating n times of this map and combining them together, we can obtain for $t \in [t_m, t_m + n\tau_d]$,

$$U_{m,n} = P_d \circ \dots \circ P_d(U_{m,0}) = P_d^n(U_{m,0}), \quad (3.3)$$

where $U_{m,i} := (u_N^T(t_m + ihN), \dots, u_0^T(t_m + ihN))^T \in \mathbb{R}^{d(N+1)}$. So the local map for the time Δt is defined as $P_{\Delta t} : \mathbb{R}^{d(N+1)} \rightarrow \mathbb{R}^{d(N+1)}$, which can be represented as

$$U_{m,n+\Delta N} = P_{\Delta t}(U_{m,n}), \quad (3.4)$$

where $U_{m,n+\Delta N} := (u_N^T(t_m + h(nN + \Delta N))^T, \dots, u_0^T(t_m + h(nN + \Delta N))^T \in \mathbb{R}^{d(N+1)}$ and $\Delta N := \frac{\Delta t}{h}$. Thus combining Eqs. (3.3) and (3.4) can construct the Poincaré map P based on T

$$U_{m,n+\Delta N} = P(U_{m+1,0}) = P_{\Delta t} \circ P_d^n(U_{m,0}), \quad (3.5)$$

where $U_{m,n+\Delta N} = U_{m+1,0}$. Once an arbitrary perturbation δU is applied, the variational equation can be written as

$$\delta U_{m+1,0} = \sum_{i=1}^{N+1} \frac{\partial P(U_{m,0})}{\partial u_{i-1}(t_m)} \delta u_{i-1}(t_m), \quad (3.6)$$

where $\delta U_{m,0} := (\delta u_N^T(t_m), \dots, \delta u_1^T(t_m), \delta u_0^T(t_m))^T \in \mathbb{R}^{d(N+1)}$, and $\delta u_i(t) := \delta u(t - \tau_d^i)$, $i = 0, \dots, N$. In fact, Eq. (3.6) can be obtained from discretising the continuous variational equation of system (2.4), and its form can be obtained as

$$\frac{d}{dt} \delta u_0(t) = \frac{\partial f_j(t, u_0(t), u_N(t))}{\partial u_0} \delta u_0(t) + \frac{\partial f_j(t, u_0(t), u_N(t))}{\partial u_N} \delta u_N(t), \quad (3.7)$$

with a suitable initial function ϕ_δ satisfying that there exists a sufficiently small ϵ , such that $\phi_\delta(t_1) = (\epsilon, 0, \dots, 0)^T \in \mathbb{R}^d$ and $\phi_\delta(t) = (0, \dots, 0)^T \in \mathbb{R}^d$ for $t \in [t_1 - \tau_d, t_1)$, and

$$\begin{cases} j = 1, & \text{if } H(u_0(t), e) > 0, \\ j = 2, & \text{if } H(u_0(t), e) < 0, \\ u_0(t^+) = u_0(t^-), & \text{if } H(u_0(t), e) = 0. \end{cases}$$

Linearising Eq. (3.7) in the interval $[t_m, t_m + n\tau_d]$ by using the modified Euler integration, it gives

$$\begin{aligned} \delta u_0(t_m + lh) &= \delta u_0(t_m + (l-1)h) \\ &+ \frac{h}{2} [A_{m,l} \delta u_0(t_m + (l-1)h) + B_{m,l} \delta u_0(t_m - (N-l+1)h)] \\ &+ \frac{h}{2} [A_{m,l+1} \delta u_0(t_m + lh) + B_{m,l+1} \delta u_0(t_m - (N-l)h)], \end{aligned} \quad (3.8)$$

where $l = 1, \dots, N, \dots, nN + \Delta N$, $A_{m,l} = \frac{\partial f_j(u_0(t), u_N(t))}{\partial u_0} \Big|_{t=t_m+h(l-1)}$, $B_{m,l} = \frac{\partial f_j(u_0(t), u_N(t))}{\partial u_N} \Big|_{t=t_m+h(l-1)}$ and $m \in \mathbb{Z}^+$. Rewriting Eq. (3.8) in a matrix form gives

$$\begin{bmatrix} \delta u_N(t_m + lh) \\ \vdots \\ \delta u_1(t_m + lh) \\ \delta u_0(t_m + lh) \end{bmatrix} = M_{m,l} \begin{bmatrix} \delta u_N(t_m + (l-1)h) \\ \vdots \\ \delta u_1(t_m + (l-1)h) \\ \delta u_0(t_m + (l-1)h) \end{bmatrix}, \quad (3.9)$$

where

$$M_{m,l} = \hat{M}_{m,l} \tilde{M}_{m,l},$$

$$\hat{M}_{m,l} = \begin{bmatrix} I & \cdots & 0 & 0 \\ \vdots & \ddots & \vdots & \vdots \\ 0 & \cdots & I & 0 \\ -\frac{h}{2}B_{m,l+1} & \cdots & 0 & I - \frac{h}{2}A_{m,l+1} \end{bmatrix}^{-1},$$

and

$$\tilde{M}_{m,l} = \begin{bmatrix} 0 & I & \cdots & 0 \\ \vdots & \vdots & \ddots & \vdots \\ 0 & 0 & \cdots & I \\ \frac{h}{2}B_{m,l} & 0 & \cdots & I + \frac{h}{2}A_{m,l} \end{bmatrix}.$$

By using the map (3.2), the matrix form of the variational equation (3.9) can be rewritten as

$$\delta U_{m,N} = M_{m,N} \circ \cdots \circ M_{m,1} \delta U_{m,0}.$$

Since we have n maps, combining all the maps for the interval $[t_m, t_m + T]$ gives

$$\delta U_{m,n} = M_{m,nN} \circ \cdots \circ M_{m,2} \circ M_{m,1} \delta U_{m,0}.$$

In addition, the map $P_{\Delta t}$ for the interval $[t_m + n\tau_d, t_m + T]$ can be written as

$$\delta U_{m+1,0} = M_{m,nN+\Delta N} \circ \cdots \circ M_{m,nN} \delta U_{m,n}. \quad (3.10)$$

Finally, the variational equation can be obtained as

$$\delta U_{m+1,0} = M_m \delta U_{m,0}, \quad (3.11)$$

where $M_m = M_{m,nN+\Delta N} \circ \cdots \circ M_{m,nN} \circ \cdots \circ M_{m,1}$ is the approximation of Jacobian matrix of the Poincaré map P .

Similarly, for the system with a large delay time, e.g. $\tau_d \geq T$, the solution of system (2.4) can be approximated by N samples at the step $h = \frac{\tau_d}{N}$ by using numerical integration, which can be consider as a special case of the nonsmooth system with a small delay time ($0 < \tau_d < T$) when $n = 0$. Let $N_T = \frac{T}{h}$ be the sample number for one period T , construct the map P_d , and combine all the linearised maps at the interval $[t_m, t_m + T]$. Finally, we can obtain the same variational equation as Eq. (3.11) and the Jacobian matrix of the Poincaré map P .

4. Modifying the algorithm on the discontinuous condition

In this section, we will discuss a special phenomenon of the impact oscillator, the so-called grazing event. Since the system has rich complex dynamics when it experiences grazing [5, 37], a careful consideration in calculating this discontinuous moment is required. In addition, the global error of our proposed algorithm will depend on the accuracy of the switching function, as the error in the switching boundary could be accumulated leading to unexpected large global error. Therefore, during the grazing event, we need to modify our proposed algorithm in Section 3 by considering two grazing cases illustrated in Fig. 4.1.

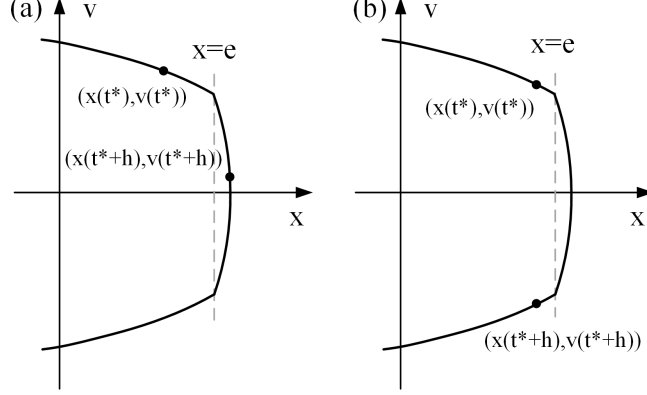


Figure 4.1: (a) Case 1: for $t = t^* > 0$, such that $H_1 := H(u_0(t^*), e) < 0$ and $H_2 := H(u_0(t^* + h), e) > 0$ (or $H_1 > 0$ and $H_2 < 0$). (b) Case 2: for $t = t^* > 0$, and there exists $\delta t \in (0, h)$, such that $H_1 := H(u_0(t^*), e) < 0$, $H_2 := H(u_0(t^* + h), e) < 0$ and $H_{cr,1} := H(u_0(t^* + \delta t), e) = 0$ (or $H_1 > 0$, $H_2 > 0$ and $H_{cr,1} = 0$).

4.1. Case 1

For Case 1, we assume that there exists $l^* \in \mathbb{Z}^+$, $t^* := t_m + (l^* - 1)h$ satisfying that for $t = t^* > 0$, $H_1 := H(u_0(t^*), e) < 0$ and $H_2 := H(u_0(t^* + h), e) > 0$, or $H_1 > 0$, $H_2 < 0$, and $H_{cr,1} := H(u_0(t^* + \delta t), e) = 0$. In order to guarantee the order of convergence of our proposed algorithm to $O(h^2)$, the crossing moment δt needs to be estimated first. Since $\delta t < h$, $H_{cr,1} = 0$ can be linearised as

$$H_{cr,1} \approx H(u(t^*) + \dot{u}(t^*)\delta t, e) \approx H_1 + \frac{d}{du}H_1[\dot{u}(t^*)\delta t] = 0,$$

then we have

$$\delta t = \frac{-H_1}{\frac{d}{du}H_1[\dot{u}(t^*)]}. \quad (4.1)$$

Once δt is calculated, the discontinuous time $t^* + \delta t$ can be obtained, and the variational equation for the discontinuous moment can be written as

$$\begin{aligned} \delta u_0(t^* + \delta t) &= \delta u_0(t^*) + \frac{\delta t}{2}[A_{m,l^*}\delta u_0(t^*) + B_{m,l^*}\delta u_N(t^*)] \\ &\quad + \frac{\delta t}{2}[A_{m,l^*}^{\delta t}\delta u_0(t^* + \delta t) + B_{m,l^*}^{\delta t}\delta u_N(t^* + \delta t)], \end{aligned} \quad (4.2)$$

where $A_{m,l^*}^{\delta t} = \frac{\partial f_j(u_0(t), u_N(t))}{\partial u_0} \Big|_{t=t_m^- + h(l^* - 1) + \delta t}$, $B_{m,l^*}^{\delta t} = \frac{\partial f_j(u_0(t), u_N(t))}{\partial u_N} \Big|_{t=t_m^- + h(l^* - 1) + \delta t}$ and $l^* = 1, \dots, N, \dots, nN + \Delta N$. Thus the local map during the interval $[t^*, t^* + \delta t]$ can be written as

$$\begin{bmatrix} \delta u_N(t^* + \delta t) \\ \vdots \\ \delta u_1(t^* + \delta t) \\ \delta u_0(t^* + \delta t) \end{bmatrix} = M_{m,l^*}^{\delta t} \begin{bmatrix} \delta u_N(t^*) \\ \vdots \\ \delta u_1(t^*) \\ \delta u_0(t^*) \end{bmatrix}, \quad (4.3)$$

where

$$M_{m,l^*}^{\delta t} = \hat{M}_{m,l^*}^{\delta t} \tilde{M}_{m,l^*}^{\delta t},$$

$$\hat{M}_{m,l^*}^{\delta t} := \begin{bmatrix} I & \cdots & 0 & 0 \\ \vdots & \ddots & \vdots & \vdots \\ 0 & \cdots & I & 0 \\ -\frac{\delta t}{2}B_{m,l^*}^{\delta t} & \cdots & 0 & I - \frac{\delta t}{2}A_{m,l^*}^{\delta t} \end{bmatrix}^{-1},$$

$$\tilde{M}_{m,l^*}^{\delta t} := \begin{bmatrix} 0 & I & \cdots & 0 \\ \vdots & \vdots & \ddots & \vdots \\ 0 & 0 & \cdots & I \\ \frac{\delta t}{2}B_{m,l^*} & 0 & \cdots & I + \frac{\delta t}{2}A_{m,l^*} \end{bmatrix},$$

$A_{m,l^*} = \frac{\partial f_j(u_0(t), u_N(t))}{\partial u_0} \Big|_{t=t_m+h(l^*-1)}$ and $B_{m,l^*} = \frac{\partial f_j(u_0(t), u_N(t))}{\partial u_N} \Big|_{t=t_m+h(l^*-1)}$. It is worth noting that $\delta u_i(t^* + \delta t)$ can be approximated through linear interpolation based on the historical data obtained from the delayed time interval which also includes the grazing data.

Similarly, for the time interval $[t^* + \delta t, t^* + h]$, we can obtain

$$\begin{bmatrix} \delta u_N(t^* + h) \\ \vdots \\ \delta u_1(t^* + h) \\ \delta u_0(t^* + h) \end{bmatrix} = \bar{M}_{m,l^*}^h \begin{bmatrix} \delta u_N(t^* + \delta t) \\ \vdots \\ \delta u_1(t^* + \delta t) \\ \delta u_0(t^* + \delta t) \end{bmatrix}, \quad (4.4)$$

where $\bar{M}_{m,l^*}^h := \hat{M}_{m,l^*}^h \tilde{M}_{m,l^*}^h$,

$$\tilde{M}_{m,l^*}^h := \begin{bmatrix} 0 & I & \cdots & 0 \\ \vdots & \vdots & \ddots & \vdots \\ 0 & 0 & \cdots & I \\ \frac{h-\delta t}{2}B_{m,l^*}^{\delta t} & 0 & \cdots & I + \frac{h-\delta t}{2}A_{m,l^*}^{\delta t} \end{bmatrix}$$

and

$$\hat{M}_{m,l^*}^h := \begin{bmatrix} I & \cdots & 0 & 0 \\ \vdots & \ddots & \vdots & \vdots \\ 0 & \cdots & I & 0 \\ -\frac{h-\delta t}{2}B_{m,l^*+1} & \cdots & 0 & I - \frac{h-\delta t}{2}A_{m,l^*+1} \end{bmatrix}^{-1}.$$

Finally, we have

$$\begin{bmatrix} \delta u_N(t^* + h) \\ \vdots \\ \delta u_1(t^* + h) \\ \delta u_0(t^* + h) \end{bmatrix} = \bar{M}_{m,l^*}^h M_{m,l^*}^{\delta t} \begin{bmatrix} \delta u_N(t^*) \\ \vdots \\ \delta u_1(t^*) \\ \delta u_0(t^*) \end{bmatrix}. \quad (4.5)$$

Therefore, when Case 1 occurs, $\bar{M}_{m,l^*}^h M_{m,l^*}^{\delta t}$ should be inserted between M_{m,l^*+1} and M_{m,l^*} for the time

interval $[t^*, t^* + h]$ in Eq. (3.10).

4.2. Case 2

If δt is the crossing moment for Case 2 which can be calculated based on Eq. (4.1), δt^* is defined as the moment satisfying $H_{\max} := H(u(t^* + \delta t + \delta t^*)) = \max_{t \in [t^*, t^* + h]} H(u(t), e)$, and $\delta \bar{t}$ is the moment that satisfies $H_{cr,2} := H(u(t^* + \delta t_g)) = 0$, where $\delta t_g := \delta t + \delta t^* + \delta \bar{t}$. The estimation of δt is similar to Eq. (4.1). From a computational point of view, Case 2 can be triggered either by (i) $H_1 < 0$, $H_2 > 0$, $\frac{d}{dt}H_1 > 0$, $\frac{d}{dt}H_2 > 0$ and $0 < \delta t_g < h$, or (ii) $H_1 > 0$, $H_2 < 0$, $\frac{d}{dt}H_1 < 0$, $\frac{d}{dt}H_2 < 0$ and $0 < \delta t_g < h$.

Since

$$\frac{d}{dt}H_{\max} \approx \frac{d}{du}H_{cr,1}[\dot{u}(t^* + \delta t) + \ddot{u}(t^* + \delta t)\delta t^*] + \frac{d^2}{du^2}H_{cr,1}[\dot{u}^2(t^* + \delta t)\delta t^*] = 0,$$

we have

$$\delta t^* = \frac{-\frac{d}{du}H_{cr,1}[\dot{u}(t^* + \delta t)]}{\frac{d}{du}H_{cr,1}[\dot{u}(t^* + \delta t)] + \frac{d^2}{du^2}H_{cr,1}[\dot{u}^2(t^* + \delta t)]}. \quad (4.6)$$

Also, we have

$$\begin{aligned} H_{cr,2} &\approx H_{\max} + \frac{d}{du}H_{\max}[\dot{u}(t^* + \delta t + \delta t^*)]\delta \bar{t} \\ &\approx H_{cr,1} + \frac{d}{du}H_{cr,1}[\dot{u}(t^* + \delta t)]\delta t^* \\ &\quad + \left[\frac{d}{du}H_{cr,1} + \frac{d^2}{du^2}H_{cr,1}[\dot{u}(t^* + \delta t)\delta t^*] \right] [\dot{u}(t^* + \delta t) + \ddot{u}(t^* + \delta t)\delta t^*]\delta \bar{t} = 0, \end{aligned}$$

which gives

$$\begin{aligned} \delta \bar{t} &= - \left[H_{cr,1} + \frac{d}{du}H_{cr,1}[\dot{u}(t^* + \delta t)]\delta t^* \right] \left[\frac{d^2}{du^2}H_{cr,1} \right. \\ &\quad \left. + \frac{d^2}{du^2}H_{cr,1}[\dot{u}(t^* + \delta t)\delta t^*] \right] [\dot{u}(t^* + \delta t) + \ddot{u}(t^* + \delta t)\delta t^*]^{-1}. \end{aligned} \quad (4.7)$$

Therefore, for the time interval $[t^*, t^* + \delta t]$, its variational equation can be written as

$$\begin{bmatrix} \delta u_N(t^* + \delta t) \\ \vdots \\ \delta u_1(t^* + \delta t) \\ \delta u_0(t^* + \delta t) \end{bmatrix} = M_{m,l^*}^{\delta t} \begin{bmatrix} \delta u_N(t^*) \\ \vdots \\ \delta u_1(t^*) \\ \delta u_0(t^*) \end{bmatrix}, \quad (4.8)$$

For the period $[t^* + \delta t, t^* + \delta t_{graz}]$,

$$\begin{bmatrix} \delta u_N(t^* + \delta t_{graz}) \\ \vdots \\ \delta u_1(t^* + \delta t_{graz}) \\ \delta u_0(t^* + \delta t_{graz}) \end{bmatrix} = M_{m,l^*}^{\delta t_{graz}} \begin{bmatrix} \delta u_N(t^* + \delta t) \\ \vdots \\ \delta u_1(t^* + \delta t) \\ \delta u_0(t^* + \delta t) \end{bmatrix}, \quad (4.9)$$

where

$$M_{m,l^*}^{\delta t_{graz}} := \hat{M}_{m,l^*}^{\delta t_{graz}} \tilde{M}_{m,l^*}^{\delta t_{graz}},$$

$$\hat{M}_{m,l^*}^{\delta t_{graz}} := \begin{bmatrix} I & \cdots & 0 & 0 \\ \vdots & \ddots & \vdots & \vdots \\ 0 & \cdots & I & 0 \\ -\frac{\delta t^* + \bar{\delta} t}{2} B_{m,l^*}^{\delta t_{graz}} & \cdots & 0 & I - \frac{\delta t^* + \bar{\delta} t}{2} A_{m,l^*}^{\delta t_{graz}} \end{bmatrix}^{-1},$$

$$\tilde{M}_{m,l^*}^{\delta t_{graz}} := \begin{bmatrix} 0 & I & \cdots & 0 \\ \vdots & \vdots & \ddots & \vdots \\ 0 & 0 & \cdots & I \\ \frac{\delta t^* + \bar{\delta} t}{2} B_{m,l^*}^{\delta t} & 0 & \cdots & I + \frac{\delta t^* + \bar{\delta} t}{2} A_{m,l^*}^{\delta t} \end{bmatrix},$$

$A_{m,l^*}^{\delta t_{graz}} = \frac{\partial f_j(u_0(t), u_N(t))}{\partial u_0} \Big|_{t=t_m^- + h(l^* - 1) + \delta t_{graz}}$ and $B_{m,l^*}^{\delta t_{graz}} = \frac{\partial f_j(u_0(t), u_N(t))}{\partial u_N} \Big|_{t=t_m^- + h(l^* - 1) + \delta t_{graz}}$. For the period $[t^* + \delta t_{graz}, t^* + h]$,

$$\begin{bmatrix} \delta u_N(t^* + h) \\ \vdots \\ \delta u_1(t^* + h) \\ \delta u_0(t^* + h) \end{bmatrix} = \bar{M}_{m,l^*}^h \begin{bmatrix} \delta u_N(t^* + \delta t_{graz}) \\ \vdots \\ \delta u_1(t^* + \delta t_{graz}) \\ \delta u_0(t^* + \delta t_{graz}) \end{bmatrix}, \quad (4.10)$$

where

$$\bar{M}_{m,l^*}^h = \hat{M}_{m,l^*}^h \tilde{M}_{m,l^*}^h,$$

$$\hat{M}_{m,l^*}^h := \begin{bmatrix} I & \cdots & 0 & 0 \\ \vdots & \ddots & \vdots & \vdots \\ 0 & \cdots & I & 0 \\ -\frac{h - \delta t_{graz}}{2} B_{m,l^*+1} & \cdots & 0 & I - \frac{h - \delta t_{graz}}{2} A_{m,l^*+1} \end{bmatrix}^{-1}$$

and

$$\tilde{M}_{m,l^*}^h := \begin{bmatrix} 0 & I & \cdots & 0 \\ \vdots & \vdots & \ddots & \vdots \\ 0 & 0 & \cdots & I \\ \frac{h - \delta t_{graz}}{2} B_{m,l^*}^{\delta t_{graz}} & 0 & \cdots & I + \frac{h - \delta t_{graz}}{2} A_{m,l^*}^{\delta t_{graz}} \end{bmatrix}.$$

Finally, we have

$$\begin{bmatrix} \delta u_N(t^* + h) \\ \vdots \\ \delta u_1(t^* + h) \\ \delta u_0(t^* + h) \end{bmatrix} = \bar{M}_{m,l^*}^h M_{m,l^*}^{\delta t_{graz}} M_{m,l^*}^{\delta t} \begin{bmatrix} \delta u_N(t^*) \\ \vdots \\ \delta u_1(t^*) \\ \delta u_0(t^*) \end{bmatrix}, \quad (4.11)$$

Thus, once Case 2 is encountered, $\bar{M}_{m,l^*}^h M_{m,l^*}^{\delta t_{graz}} M_{m,l^*}^{\delta t}$ should be inserted between M_{m,l^*+1} and M_{m,l^*} in Eq. (3.10) for the time interval $[t^*, t^* + h]$.

From the discussion above, we can obtain an accurate Jacobian matrix for the Poincaré map (2.5). In the next section, we will discuss the convergence of eigenvalues of the Jacobian matrix when a perturbation is introduced in order to ensure the accuracy of our proposed method.

5. Convergence analysis

5.1. Properties of the evaluation operator

According to [31, 38], the eigenvalues of the Jacobian matrix for the Poincaré map can be considered as the spectral of operator. So we will study the Poincaré map of Eq. (3.7) and its relevant operator.

For the space \mathbb{C}^d , assume $\mathbb{P} := [t_1, t_1 + \Delta T]$, which is an bounded interval of \mathbb{R} and $\Delta T < +\infty$. $C(\mathbb{P}, \mathbb{C}^d)$ denotes the Banach space with all bounded continuous functions from \mathbb{P} to \mathbb{C}^d with the norm $\|u\|_C = \max_{t \in \mathbb{P}} |u(t)|$, where $u \in C(\mathbb{P}, \mathbb{C}^d)$ and $|\cdot|$ is a given norm on \mathbb{C}^d .

Now, we rewrite Eq. (3.7) as

$$\begin{cases} \frac{d}{dt} \delta u_0(t) = F(t, \delta u_0(t), \delta u_N(t)), & \text{where } t \in \mathbb{P} \text{ and } F \in C(\mathbb{P}, \mathbb{C}^d), \\ \delta u_0(t) = \phi_\delta(t), & \text{where } t \in [t_1 - \tau_d, t_1] \text{ and } \phi_\delta \in C([t_1 - \tau_d, t_1], \mathbb{C}^d), \end{cases} \quad (5.1)$$

where ϕ_δ is defined in Eq. (3.7). Here, we assume $\delta u_d(t) = \delta u_N(t)$, and F can be written as

$$F(t, \delta u_0(t), \delta u_d(t)) = F_{j,1}(t) \delta u_0(t) + F_{j,2}(t) \delta u_d(t), \quad (5.2)$$

where

$$\begin{cases} j = 1, & \text{if } H(u_0(t), e) > 0, \\ j = 2, & \text{if } H(u_0(t), e) < 0, \\ F(t^-, \delta u_0(t^-), \delta u_d(t^-)) = F(t^+, \delta u_0(t^+), \delta u_d(t^+)), & \text{if } H(u_0(t), e) = 0, \end{cases}$$

$$F_{j,1}(t) := \frac{\partial f_j(t, u_0(t), u_d(t))}{\partial u_0}, \text{ and } F_{j,2}(t) := \frac{\partial f_j(t, u_0(t), u_d(t))}{\partial u_d}.$$

According to [30], nonautonomous delayed dynamical system can be represented as an evolution operator. So, for any $t_1 \in \mathbb{P}$ and sufficiently small $h > 0$, we have

$$U(t_1 + h, t_1) \phi_\delta = \delta u_0(t_1 + h), \quad (5.3)$$

where $\delta u_0(t_1 + h)$ is the solution of Eq. (5.1) at $t = t_1 + h$. For any time $t = t_1 + N_t h$, $\forall N_t \in \mathbb{Z}^+$, $\delta u_0(t)$ can be written as

$$\delta u_0(t) = U(t_1 + h N_t, t_1 + h(N_t - 1)) \cdots U(t_1 + 2h, t_1 + h) U(t_1 + h, t_1) \phi_\delta.$$

Next, we will construct the approximation operator with finite dimension for the evolution operator $U(t_1 + h, t_1)$. In order to simplify our discussion, we define the following operators

$$\mathcal{P} := C([t_1 - \tau_d, t_1], \mathbb{C}^d),$$

and

$$\mathcal{P}^+ := C([t_1, t_1 + h], \mathbb{C}^d),$$

their relevant norms

$$\|\cdot\| := \max_{t \in [t_1 - \tau_d, t_1]} |\cdot|,$$

and

$$\|\cdot\|^+ := \max_{t \in [t_1, t_1 + h]} |\cdot|,$$

and the space

$$\mathcal{P}^* := C([t_1 - \tau_d, t_1 + h], \mathbb{C}^d),$$

with the map $L : \mathcal{P} \times \mathcal{P}^+ \rightarrow \mathcal{P}^*$ satisfying

$$L(\phi_\delta, z)(\eta) = \begin{cases} \phi_\delta(t_0) + \int_{t_1}^\eta z(\theta) d\theta, & \text{if } \eta \in [t_1, t_1 + h], \\ \phi_\delta(\eta), & \text{if } \eta \in [t_1 - \tau_d, t_1]. \end{cases}$$

According to [30], the map L can be divided into two operators $L_1 : \mathcal{P} \rightarrow \mathcal{P}^*$ and $L_2 : \mathcal{P}^+ \rightarrow \mathcal{P}^*$ with

$$L(\phi_\delta, \omega) = L_1\phi_\delta + L_2\omega, \tag{5.4}$$

where $(\phi_\delta, \omega) \in \mathcal{P} \times \mathcal{P}^+$, $L_1\phi_\delta = L(\phi_\delta, 0)$ and $L_2\omega = L(0, \omega)$.

In addition, the linear operator $\Theta : \mathcal{P}^* \rightarrow \mathcal{P}^+$ satisfies

$$\Theta v(t) = F(t, v(t), v_d(t)), \tag{5.5}$$

where $v, v_d \in \mathcal{P}^*$ and $t \in [t_1, t_1 + h]$, and it has a fixed point $\omega^* \in \mathcal{P}^+$ which is the solution of the following equation

$$\omega^* = \Theta L(\phi_\delta, \omega^*). \tag{5.6}$$

It is obvious that if the initial problem (5.1) has a solution in $[t_1, t_1 + h]$, Eq. (5.6) will have a solution. So ω^* satisfies

$$U(t_1 + h, t_1)\phi_\delta = L(\phi_\delta, \omega^*). \tag{5.7}$$

According to Eq. (5.4), Eq. (5.6) can be rewritten as

$$(I_{\mathcal{P}^+} - \Theta L_2)\omega^* = \Theta L_1\phi_\delta \tag{5.8}$$

where $I_{\mathcal{P}^+}$ is the identity operator for the space \mathcal{P}^+ . Therefore, we can derive the following properties for the operators ΘL_1 and ΘL_2 .

Proposition 1. If the operator Θ is defined as Eq. (5.5), it is a bounded linear operator with $v(t) \in \mathcal{P}^*$.

Proof. Let $v_1, v_2 \in \mathcal{P}^*$, where

$$\Theta v_1(t) = F(t, v_1(t), v_1(t - \tau_d)),$$

and

$$\Theta v_2(t) = F(t, v_2(t), v_2(t - \tau_d)).$$

Then we can obtain

$$\begin{aligned} \|\Theta(v_1 + v_2)\| &\leq |F_{j,1}^{\tau}(t)v_1(t) + F_{j,2}^{\tau}(t)v_1(t - \tau_d)| + |F_{j,1}(t)v_2(t) + F_{j,2}(t)v_2(t - \tau_d)| \\ &= \|\Theta v_1\| + \|\Theta v_2\| \end{aligned}$$

In addition, according to Eq. (5.2), there must exist a positive constant B_{Θ} satisfying that, for any $v \in \mathcal{P}^*$, $\|\Theta v\| \leq B_{\Theta}\|v\|$. Therefore, the operator Θ is bounded and linear in the space. \square

Proposition 2. If L_1 and L_2 are defined as Eq. (5.4), ΘL_1 and ΘL_2 are bounded linear operators with regard to $\omega \in \mathcal{P}^+$.

Proof. For $\forall \phi_{\delta}$, there exists $\omega_0, \omega_1, \omega_2 \in \mathcal{P}^+$ such that $\Theta L(\phi_{\delta}, \omega_0) = \omega_0$ and $\omega_0 = \omega_1 + \omega_2$. So we have

$$\begin{aligned} \Theta L(\phi_{\delta}, \omega_0) &= \Theta[L_1(\phi_{\delta}, \omega_1) + L_2\omega_2] \\ &= \Theta L_1(\phi_{\delta}) + \Theta L_2\omega_1 + \Theta L_2\omega_2 \\ &= \Theta L_1(\phi_{\delta}) + \Theta L_2(\omega_1 + \omega_2). \end{aligned}$$

According to the Eqs. (5.5)-(5.7), if $\Theta L(0, \omega) = \omega$ (where $\omega \in \mathcal{P}^+$) holds, $L(0, \omega)$ must be the solution of the following system

$$\begin{cases} \frac{d}{dt}\delta u_0(t) = F(t, \delta u_0(t), \delta u_d(t)), \\ \delta u_0(s) = 0, \end{cases} \quad (5.9)$$

where $F \in C(\mathbb{P}, \mathbb{R}^d)$ and $s \in [t_1 - \tau_d, t_1]$. Then for any $\omega \in \mathcal{P}^+$, it gives $\|\Theta L_2\omega\| = \|\omega\|$, so ΘL_2 is bounded.

Let $\phi_{\delta,1}, \phi_{\delta,2} \in \mathcal{P}$, and for $\phi_{\delta,1} + \phi_{\delta,2}$, there exists $\omega \in \mathcal{P}^+$ such that $\Theta L(\phi_{\delta,1} + \phi_{\delta,2}, \omega) = \omega$. Also, there exists $\omega_1, \omega_2 \in \mathcal{P}^+$, such that $\omega = \omega_1 + \omega_2$. Then we have

$$\begin{aligned} L(\phi_{\delta,1} + \phi_{\delta,2}, \omega) &= L(\phi_{\delta,1}, \omega_1) + L(\phi_{\delta,2}, \omega_2) \\ &= L_1\phi_{\delta,1} + L_2\omega_1 + L_1\phi_{\delta,2} + L_2\omega_2 \\ &= L_1(\phi_{\delta,1} + \phi_{\delta,2}) + L_2\omega \end{aligned}$$

Since

$$\Theta[L_1\phi_{\delta,1} + L_2\omega_1 + L_1\phi_{\delta,2} + L_2\omega_2] = \Theta L_1\phi_{\delta,1} + \Theta L_1\phi_{\delta,2} + \Theta L_2\omega$$

and

$$\Theta[L_1(\phi_{\delta,1} + \phi_{\delta,2}) + L_2\omega] = \Theta L_1(\phi_{\delta,1} + \phi_{\delta,2}) + \Theta L_2\omega,$$

ΘL_1 is a bounded linear operator. \square

5.2. Approximation of the evaluation operator

Since the system (5.1) can be approximated by large finite ODE systems, the approximated operators are constructed through discretisation by introducing the relevant discrete space of \mathcal{P} and \mathcal{P}^+ along with

the following operators. As large finite ODE systems can be obtained from the modified Euler integration, we can adopt linear interpolation to discretise the space \mathcal{P} and \mathcal{P}^+ .

First of all, based on the time step h , consider the mesh $\Lambda_{N+1} := (t_1 - Nh, \dots, t_1 - h, t_1)$ in $[t_1 - \tau_d, t_1]$, we can construct a restriction operator $r_h : \mathcal{P} \rightarrow \mathcal{P}_{N+1} := \mathbb{C}^{d(N+1)}$ on Λ_{N+1} , such that $r_h \phi_\delta \in \mathcal{P}_{N+1}$, where $r_h \phi_\delta^i = \phi_\delta(t_1 - (N+1-i)h) \in \mathbb{C}^d$. In addition, there exists a prolongation operator on the mesh Λ_{N+1} such that for any $\varpi_{N+1} := (\varpi^T(t_1 - Nh), \dots, \varpi^T(t_1))^T \in \mathcal{P}_{N+1}$, where $\varpi \in \mathcal{P}$, $\bar{r}_h : t \in [t_1 - \tau_d, t_1] \rightarrow \bar{r}_h(t) \in \mathbb{C}^{1 \times d(N+1)}$, $\bar{r}_h(t_1 - (N+1-i)h)\varpi_{N+1} = \varpi(t_1 - (N+1-i)h)$, $i \in \mathbb{Z}[1, N+1]$, and $\bar{r}_h(t)\varpi_{N+1}$ is a polynomial with a degree less than or equal to 2.

Similarly, consider the mesh $\Lambda_{K+1} := (t_1, t_1 + h_s, \dots, t_1 + Kh_s)$ in $[t_1, t_1 + h]$, where $0 < h_s < h$, $K = h/h_s$, the space \mathcal{P}^+ can be discretised by the restriction operator $R_{h_s} : \mathcal{P}^+ \rightarrow \mathcal{P}_{K+1}^+ := \mathbb{C}^{d(K+1)}$ on the mesh Λ_{K+1} such that $R_{h_s} \psi \in \mathcal{P}_{K+1}^+$, where $R_{h_s} \psi^i = \psi(t_1 + (i-1)h_s) \in \mathbb{C}^d$. Therefore, we can construct a relevant prolongation operator on the mesh Λ_{K+1} as follows. For any $\varpi_{K+1} := (\varpi^T(t_1), \dots, \varpi^T(t_1 + Kh_s)) \in \mathcal{P}_{K+1}^+$, where $\varpi \in \mathcal{P}^+$, $\bar{R}_{h_s} : t \in [t_1, t_1 + h] \rightarrow \bar{R}_{h_s}(t) \in \mathbb{C}^{d(K+1)}$, such that $\bar{R}_{h_s}(t_1 + (i-1)h_s)\varpi_{K+1} = \varpi(t_1 + (i-1)h_s)$, $i \in \mathbb{Z}[1, K+1]$, and $\bar{R}_{h_s}(t)\varpi_{K+1}$ is a polynomial with degree less than or equal to $K+1$. Here, the operator $\mathfrak{L} := \bar{R}_{h_s}(t)R_{h_s}$ is a Lagrange operator [39].

Let $K = 1$ (i.e. $h_s = h$) and for any given N , the relevant approximated operator $U_{N+1,1}(t_1 + h, t_1) : \mathcal{P}_{N+1} \rightarrow \mathcal{P}_{N+1}$ satisfies

$$U_{N+1,2}(t_1 + h, t_1)\Phi = r_h L(\bar{r}_h(t - \tau_d)\Phi, \bar{R}_{h_s}(t)\Psi^*), \quad (5.10)$$

where $t \in [t_1, t_1 + h]$, $\Phi \in \mathcal{P}_{N+1}$ and $\Psi^* \in \mathcal{P}_{K+1}^+$, which is the solution of the following equation

$$\Psi^* = R_{h_s} \Theta L(\bar{r}_h(t - \tau_d)\Phi, \bar{R}_{h_s}(t)\Psi^*). \quad (5.11)$$

It is worth noting that the operator \bar{R}_{h_s} at the time interval $[t_1, t_1 + h]$ can be more accurate if the time step h is reduced.

5.3. Convergence analysis for the nonzero eigenvalues of the Jacobian matrix

In this section, we will present the convergence analysis for $0 < \tau_d < T$ only, and the proof for $\tau_d \geq T$ is similar, so will be omitted here. In order to ensure the only solution for the initial problem (5.1), we introduce the subspace \mathcal{P}_{Lip}^+ of \mathcal{P}^+ with the norm

$$\|\psi\|_{Lip}^+ = l(\psi) + \|\psi\|^+, \quad \psi \in \mathcal{P}_{Lip}^+,$$

where $l(\psi)$ is the Lipschitz constant of ψ , and the subspace \mathcal{P}_{Lip} of \mathcal{P} with the norm as

$$\|\psi\|_{Lip} = l(\psi) + \|\psi\|, \quad \psi \in \mathcal{P}_{Lip}.$$

To carry out convergence analysis for the eigenvalues of Jacobian matrix of the Poincaré map (2.5), the following lemmas are given.

Lemma 5.1. For any $\sigma_1^*, \sigma_2^* \in \mathcal{P}^+$,

$$\sigma_1^* = \mathfrak{L} \Theta L(\phi_\delta, \sigma_1^*), \quad \phi_\delta \in \mathcal{P}, \quad (5.12)$$

and

$$\sigma_2^* = \Theta L(\phi_\delta, \sigma_2^*), \quad \phi_\delta \in \mathcal{P},$$

for sufficiently small h , and we have

$$\|\sigma_1^* - \sigma_2^*\|^+ \leq c_1 h^2, \quad (5.13)$$

where c_1 is a positive constant.

Proof. Based on Theorem 3.3 in [30] and let $\sigma_1^* = \sigma_2^* + \rho^*$, we have

$$\|\rho^*\| := \|\sigma_1^* - \sigma_2^*\|^+ = \|(I_{\mathcal{P}^+} - \mathfrak{L}\Theta L_2)^{-1}\| \|(I_{\mathcal{P}^+} - \mathfrak{L})\|^+ \|\sigma_2^*\|_{Lip}^+, \quad (5.14)$$

For sufficiently small h , $\|(I_{\mathcal{P}^+} - \mathfrak{L})\|^+$ is the global error from the modified Euler integration, which satisfies

$$\|(I_{\mathcal{P}^+} - \mathfrak{L})\|^+ \leq c_2 h^2,$$

where c_2 is a positive constant. Since

$$I_{\mathcal{P}^+} - \mathfrak{L}\Theta L_2 = (I_{\mathcal{P}^+} - \Theta L_2) + (I_{\mathcal{P}^+} - \mathfrak{L})\Theta L_2,$$

and ΘL_2 is bounded, if $h \rightarrow 0$, $(I_{\mathcal{P}^+} - \mathfrak{L}\Theta L_2)^{-1} = (I_{\mathcal{P}^+} - \Theta L_2)^{-1}$. In addition, as

$$\sigma_2^* = (I_{\mathcal{P}^+_{Lip}} - \Theta L_2)^{-1} \Theta L_1 \phi_\delta, \quad (5.15)$$

and

$$\|\sigma_2^*\|_{Lip}^+ \leq \|(I_{\mathcal{P}^+_{Lip}} - \Theta L_2)^{-1}\| \|\Theta L_1\| \|\phi_\delta\|_{Lip}, \quad (5.16)$$

$\|\sigma_2^*\|_{Lip}^+$ is bounded. Thus, there must exist a positive constant c_1 for Eq. (5.14) satisfying

$$\|\rho^*\| \leq c_1 h^2.$$

□

Based on Eq. (5.10), a new operator in the interval $[t_1, t_1 + h]$ can be introduced as

$$\bar{U}_{N+1,2}(t_1 + h, t_1) = \bar{r}_h U_{N+1,2}(t_1 + h, t_1) r_h : \mathcal{P} \rightarrow \mathcal{P}, \quad (5.17)$$

which has the same geometric and partial multiplicities as the operator $U_{N+1,2}(t_1 + h, t_1)$ in Eq. (5.10). Therefore, there exists a map $\bar{U}_2(t_1 + h, t_1) : \mathcal{P} \rightarrow \mathcal{P}$ such that

$$\bar{U}_2(t_1 + h, t_1) \phi_\delta = L(\phi_\delta, \sigma^*), \quad \phi_\delta \in \mathcal{P}, \quad (5.18)$$

where $\sigma^* \in \mathcal{P}^+$ is the solution of Eq. (5.12), and $\bar{U}_{N+1,2}(t_1 + h, t_1)$ can be written as

$$\bar{U}_{N+1,2}(t_1 + h, t_1) = \mathfrak{L} \bar{U}_2(t_1 + h, t_1) \mathfrak{L}.$$

Lemma 5.2. If the operator $\bar{U}_2(t_1 + h, t_1)$ is defined as Eq. (5.18), we have

$$\|\bar{U}_2(t_1 + h, t_1) - U(t_1 + h, t_1)\| \leq c h^3, \quad (5.19)$$

where c_3 is a positive constant.

Proof. For $(\phi_\delta, \omega_1^*), (\phi_\delta, \omega_2^*) \in \mathcal{P}_{Lip}^+ \times \mathcal{P}^+$, based on Eq. (5.4), we have

$$\|\bar{U}_2(t_1 + h, t_1) - U(t_1 + h, t_1)\| = \|L(\phi_\delta, \omega_1^*) - L(\phi_\delta, \omega_2^*)\| = \|L_2(\omega_1^* - \omega_2^*)\|,$$

where

$$\omega^* = \bar{I}_{\mathcal{P}^+} \Theta L(\phi_\delta, \omega_1^*)$$

and

$$\sigma^* = \Theta L(\phi_\delta, \omega_2^*).$$

So

$$\begin{aligned} \|\bar{U}_2(t_1 + h, t_1) - U(t_1 + h, t_1)\| &= \|L_2(\omega_1^* - \omega_2^*)\| \\ &= \left\| \int_{t_1}^{t_1+h} (\omega_1^* - \omega_2^*)(t) dt \right\| = \|(\omega_1^* - \omega_2^*)\|^+ h. \end{aligned}$$

According to Eqs. (5.14) and (5.15) and the inequality (5.16), we have

$$\|\bar{U}_2(t_1 + h, t_1) - U(t_1 + h, t_1)\| \leq c_3 h^3.$$

□

It is worth noting that the evolution operator $\bar{U}_2(t_1 + ih, t_1 + (i-1)h)$, where $i = 1, \dots, \bar{N}$ and $\bar{N} := N + n + \Delta N + 1$, must have the same properties as the operator $U(t_1 + ih, t_1 + (i-1)h)$ in the inequality (5.19). Thus, Poincaré map can be constituted by combining all the evolution operators $U(t_1 + ih, t_1 + (i-1)h)$ over the entire time interval $[t_1, t_1 + T]$. As a result, the convergence problem is transferred to study the convergence of the operator $\prod_{i=1}^{\bar{N}} \bar{U}_2(t_1 + ih, t_1 + (i-1)h)$ to $U(t_1, t_1 + T)$.

Lemma 5.3. For the entire interval $[t_1, t_1 + T]$ and a sufficiently small time step h , we can obtain

$$\|U(t_1 + T, t_1) - \prod_{i=1}^{\bar{N}} \bar{U}_2(t_1 + ih, t_1 + (i-1)h)\| \leq c_4 h^2, \quad (5.20)$$

where $i = 1, 2, \dots, \bar{N}$, $\bar{N} := N + n + \Delta N + 1$, and c_4 is a positive constant.

Proof. According to Lemma 5.2, we assume that there are two positive constants M_1 and M_2 such that

$$\left\| \prod_{i=2}^{\bar{N}-1} U(t_1 + ih, t_1 + (i-1)h) \right\| \leq M_1, \quad (5.21)$$

and

$$\left\| \prod_{j=1}^{\bar{N}-1} \bar{U}_2(t_1 + jh, t_1 + (j-1)h) \right\| \leq M_2. \quad (5.22)$$

Therefore,

$$\begin{aligned}
& \left| U(t_1 + T, t_1) - \prod_{i=1}^{\bar{N}} \bar{U}_2(t_1 + ih, t_1 + (i-1)h) \right| \\
& \leq \bar{N} \prod_{i=2}^{\bar{N}-1} U(t_1 + ih, t_1 + (i-1)h) \prod_{j=1}^{\bar{N}-1} \bar{U}_2(t_1 + jh, t_1 + (j-1)h) c_3 h^3 \\
& \leq \bar{N} M_1 M_2 c_3 h^3 = \frac{T}{h} M_1 M_2 c_3 h^3 = c_4 h^2.
\end{aligned}$$

□

Combining the inequality (5.20) with the results in [31, 38] and Theorem 4.6 and 4.7 in [30], the following lemma can be obtained.

Lemma 5.4. Let $\lambda \in \mathbb{C} \setminus \{0\}$ be an isolated eigenvalue for the operator $U(t_1 + T, t_1)$ with the finite algebraic multiplicity m_a and ascent κ , and Γ be a neighborhood of λ for U on the time interval $[t_1, t_1 + T]$. For a sufficiently small h , $\bar{U}_2(t_1 + T, t_1)$ has m eigenvalues $\lambda_{2,\iota}$, where $\iota = 1, \dots, m$, and we have

$$\max_{\iota=1,\dots,m} |\lambda - \lambda_{2,\iota}| \leq c_5 h^{\frac{2}{\kappa}}, \quad (5.23)$$

where c_5 is a positive constant.

It should be noted that $\bar{U}_{N+1,2}$ and \bar{U}_2 have the same nonzero eigenvalues, geometric and partial multiplicities and eigenvectors. Hence, the following theorem is obtained.

Theorem 5.5. Let $\lambda \in \mathbb{C} \setminus \{0\}$ be an isolated eigenvalue for the operator $U(t_1 + T, t_1)$ with the finite algebraic multiplicity m_a and the ascent κ , and let Γ be a neighborhood of λ for the time interval $[t_1, t_1 + T]$. For a sufficiently small h , $\bar{U}_{N+1,2}(t_1 + T, t_1)$ has m eigenvalues $\lambda_{N+1,2,\iota}$, where $\iota = 1, \dots, m$ and we have

$$\max_{\iota=1,\dots,m} |\lambda - \lambda_{N+1,2,\iota}| \leq c_6 h^{\frac{2}{\kappa}}, \quad (5.24)$$

where c_6 is a positive constant.

For any interval $[t_m, t_m + T]$, the inequality (5.24) always exists. From the above study, we can ensure that our proposed calculation method has a good convergence rate on the nonzero characteristic multipliers of the system (5.1). So our approximation for the Jacobian matrix of the Poincaré map (2.5) is reliable. It is also worth noting that by adopting a high-order integration method (e.g. Runge-Kutta method) with a sufficiently small time step h , the approximated operator could be more accurate $O(h^4)$. If the local estimation in Section 4 is not used, the convergence of the approximated operator cannot be guaranteed as the same with the order of the numerical integration. Furthermore, if the system encounters sufficiently large number of times of grazing, the convergence rate will be lower than $O(h^2)$ due to the grazing events.

6. Calculation of the Lyapunov exponents

Since the entire motion of the system (2.4) can be represented by the Poincaré map (2.5) as

$$Y_{m+1,0} = P^m(Y_{1,0}) = P \circ \dots \circ P \circ P(Y_{1,0}), \quad (6.1)$$

where the Jaobian matrix of P^m is $\prod_{i=1}^m M_i$. According to Definition 2.1, LEs can be calculated as

$$\vartheta_i = \lim_{m \rightarrow \infty} \frac{1}{m} \ln |\lambda_i^m|, \quad i = 1, \dots, d(N+1), \quad (6.2)$$

where λ_i^m is the i^{th} eigenvalues of $\prod_{i=1}^m M_i$.

However, calculating LEs by using Eq. (6.2) will introduce an overflow problem. In detail, some elements of the Jacobian matrix will be very large for chaotic attractors, and some of them could be very small for periodic attractors, which may cause inaccurate calculation. On the other hand, calculating LEs from the Jacobian matrix directly is time-consuming as time-delayed dynamical system is high-dimensional. To overcome these issues, LEs can be computed according to the average exponent divergence rate between the basis orbit started from $Y_1(0)$ and its neighborhood orbit along the direction of $v_{1,0} = \frac{Y_{1,0}}{\|Y_{1,0}\|}$ as

$$\vartheta(Y_{1,0}, v_{1,0}) = \lim_{m \rightarrow \infty} \frac{1}{m} \ln \frac{\|\delta Y_{m,0}\|}{\|\delta Y_{1,0}\|}, \quad (6.3)$$

where $\|\delta Y_{m,0}\|$ is the norm of $\delta Y_{m,0}$ and $m \in \mathbb{Z}^+$.

Next, choose $Y_{1,0} \in \mathbb{R}^{d(N+1)}$, and its related linearly independent initial perturbed vector $(\delta Y_{1,0}^1, \delta Y_{1,0}^2, \dots, \delta Y_{1,0}^{d(N+1)})$ can be normalised as

$$(\delta v_{1,0}^1, \delta v_{1,0}^2, \dots, \delta v_{1,0}^{d(N+1)}) = \left(\frac{\delta Y_{1,0}^1}{\|\delta Y_{1,0}^1\|}, \frac{\delta Y_{1,0}^2}{\|\delta Y_{1,0}^2\|}, \dots, \frac{\delta Y_{1,0}^{d(N+1)}}{\|\delta Y_{1,0}^{d(N+1)}\|} \right). \quad (6.4)$$

Substituting the vector (6.4) to Eq. (6.1) obtains the second vector $(\delta Y_{2,0}^1, \delta Y_{2,0}^2, \dots, \delta Y_{2,0}^{d(N+1)})$, and Gram-Schmidt orthonormalization [36] can be applied to normalise the second vector, which gives a new vector $(\delta v_{2,0}^1, \delta v_{2,0}^2, \dots, \delta v_{2,0}^{d(N+1)})$. For the next iteration, the second vector will be used as the initial vector to be substituted into Eq. (6.1). Likewise, repeating m times for this process gives the m^{th} vector $(\delta Y_{m,0}^1, \delta Y_{m,0}^2, \dots, \delta Y_{m,0}^{d(N+1)})$. The steps of Gram-Schmidt orthonormalization are given as follows

$$\begin{aligned} V_{m,0}^1 &= \delta Y_{m,0}^1, \\ \delta v_{m,0}^1 &= \frac{V_{m,0}^1}{\|V_{m,0}^1\|}, \\ V_{m,0}^2 &= \delta Y_{m,0}^2 - \langle \delta Y_{m,0}^2, \delta v_{m,0}^1 \rangle \delta v_{m,0}^1, \\ \delta v_{m,0}^2 &= \frac{V_{m,0}^2(0)}{\|V_{m,0}^2\|}, \\ &\vdots \\ V_{m,0}^{d(N+1)} &= \delta Y_{m,0}^{2(N+1)} - \langle \delta Y_{m,0}^{2(N+1)}, \delta v_{m,0}^1 \rangle \delta v_{m,0}^1 - \dots \\ &\quad - \langle \delta Y_{m,0}^{d(N+1)}, \delta v_{m,0}^{d(N+1)-1} \rangle \delta v_{m,0}^{d(N+1)-1}, \\ \delta v_{m,0}^{d(N+1)} &= \frac{V_{m,0}^{d(N+1)}}{\|V_{m,0}^{d(N+1)}\|}, \end{aligned}$$

where $\|V_{m,0}^i\|$ is the norm of $V_{m,0}^i$, $\langle \delta Y_{m,0}^i, \delta v_{m,0}^{\bar{i}} \rangle$ ($i, \bar{i} = 1, 2, \dots, d(N+1)$) is a standard scalar product.

Finally, LEs can be calculated by using

$$\vartheta_i \approx \frac{1}{m} \ln \prod_{\varrho=1}^m \|V_{\varrho}^i(0)\| = \frac{1}{m} \sum_{\varrho=1}^m \ln \|V_{\varrho}^i(0)\|. \quad (6.5)$$

7. Numerical studies

In this section, we will show the effectiveness of our proposed method by studying the soft impacting system with a delayed feedback controller presented in Fig. 2.1. Since the system has many coexisting attractors when grazing is encountered [32], our control objective here is to drive the system from its current attractor to a desired one. Calculating the LEs of the system allows us to monitor the stability of the delayed feedback controller and its effective parametric regime.

Now, we consider the following parameters for the impacting system,

$$\zeta = 0.01, \quad e = 1.26, \quad a = 0.7, \quad \beta = 28 \quad \text{and} \quad \omega = 0.802,$$

at where a grazing event is encountered, and a chaotic and a period-5 attractors coexist as shown in Fig. 7.1.

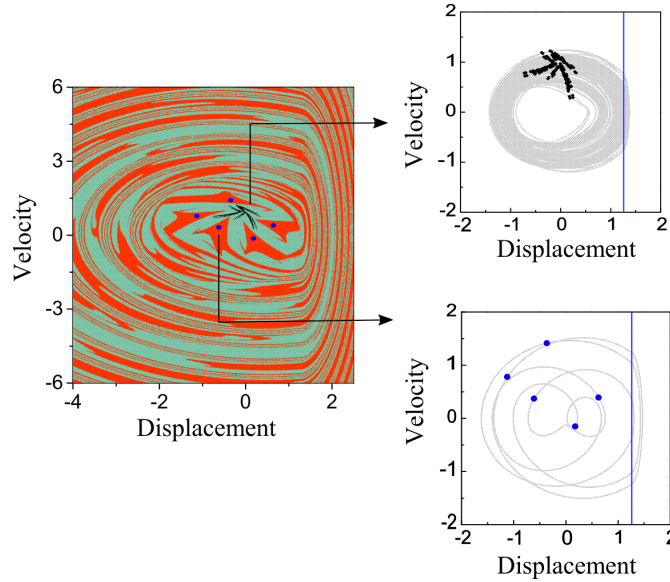


Figure 7.1: Basin of attraction of the impacting system computed for $\zeta = 0.01$, $e = 1.26$, $a = 0.7$, $\beta = 28$ and $\omega = 0.802$. Black dots denote the chaotic attractor with green basin, blue dots represent the period-5 attractor with red basin, and blue lines denote the impact boundary.

7.1. Case $\tau_d \geq T$

Fig. 7.2 presents the first example of using the delayed feedback controller (2.3) for which a large delayed time (i.e. $\tau_d \geq T$) was considered, and the control parameter k was varied from 0 to 1.4. As can be seen from Fig. 7.2(a), the largest LEs are all greater than 0 for $k \in [0, 0.04]$ and the system presents a chaotic motion as shown in Fig. 7.2(b). The phase trajectory of the chaotic motion for $k = 0.02$ is presented in Fig. 7.2(c). For $k \in (0.04, 0.055)$, the largest LEs decrease and suddenly increase to the neighbourhood of zero at $k = 0.055$ indicating a period doubling of the system. Similarly, at $k = 0.065$,

such a fluctuation is observed again. Thereafter, the largest LEs decrease dramatically, and then increase gradually from $k = 0.07$. For $k \in [0.07, 1.4]$, both LEs are below zero, and the system has period-1 response which is demonstrated by Figs. 7.2(d) and (e).

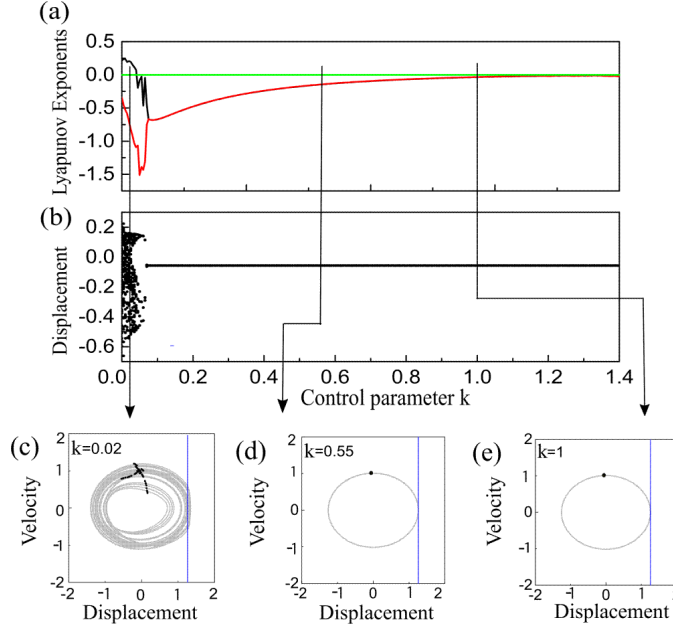


Figure 7.2: (a) LEs and (b) displacement of the impacting system under the delayed feedback controller as functions of the control parameter k . Black, red and green lines denote the two largest LEs and the zero line, respectively. Additional panels show the phase trajectories of the system calculated for (c) $k = 0.02$, (d) $k = 0.55$ and (e) $k = 1$. Black dots represent the Poincaré sections, and blue lines represent the impact boundary.

A critical issue for computing nonsmooth dynamical systems is that the accumulated computational error from the impact boundary due to grazing event could lead to inaccurate simulation. Fig. 7.3 compares the computations of the impacting system for $e = 1.2609$ controlled from a chaotic response to a period-1 response by using the delayed feedback control with and without the grazing estimation algorithm. The number of impacts as a function of time without (black line) and with (orange line) the grazing estimation algorithm is presented in Fig. 7.3(a) which were counted from $t = 9722$, and the phase trajectories from chaotic (grey line) to period-1 (red line) response were shown in Fig. 7.3(b). It can be seen from the figure that the accumulated error was built up in the number of impacts, and a clear difference can be observed from $t = 10411$. The cause of such a difference can be found from Figs. 7.3(c) and (d), at where the time histories of displacement of the impacting system were shown. As can be seen from the figures, the system with the grazing estimation algorithm was stabilised quicker than the one without the algorithm. As the modified Euler integration method was used in this work, the difference could be more significant if a higher order integration method, e.g. RungeKutta integration method, is adopted.

7.2. Case $0 < \tau_d < T$

For the case of a small time delay (i.e. $0 < \tau_d < T$), we present the example for $\tau_d = T/2$ in Fig. 7.4. It can be seen from the figures that the system has chaotic motion for $k \in [0, 0.007]$ and its largest LEs are all greater than zero (green line). For $k \in (0.007, 0.015]$, the system experiences transient periodic motion, and the relevant largest LEs are smaller than zero which is consistent with the result shown in Fig. 7.4(b)

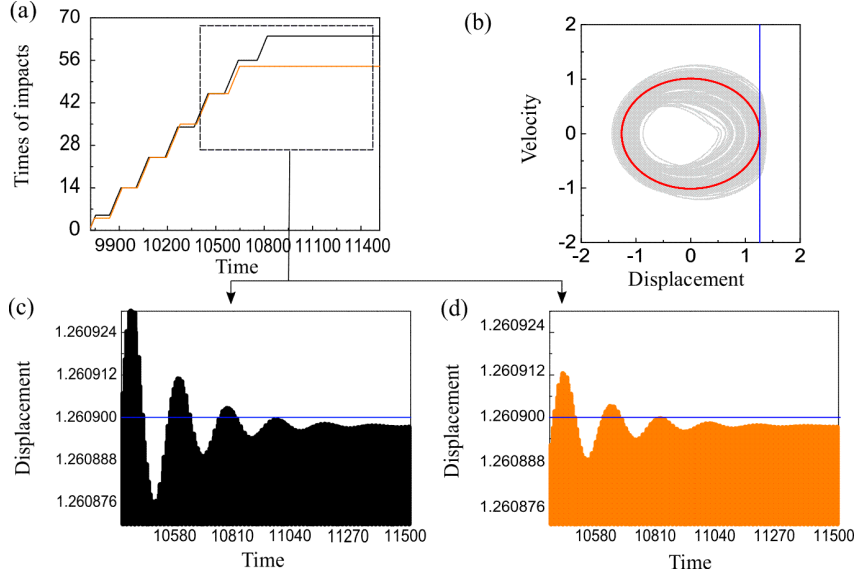


Figure 7.3: (a) Number of impacts as a function of time without (black line) and with (orange line) the grazing estimation algorithm based on the discontinuous condition calculated for $\zeta = 0.01$, $e = 1.2609$, $a = 0.7$, $\beta = 28$, $\omega = 0.802$ and $k = 1.4$. (b) Phase trajectories of the impacting system controlled from chaotic (grey line) to period-1 (red line) response. Time histories of displacement of the system (c) without and (d) with the algorithm are presented, and blue lines indicate the discontinuous boundary.

indicating several alternations between chaotic and periodic motions. At $k = 0.016$, the system has a very small chaotic regime and bifurcates into a non-impact period-1 response immediately lasting until $k = 0.0425$ at where another chaotic regime is encountered. For $k \in [0.0425, 0.045]$, the system has chaotic response in most of the regime, but has a small window of period-3 response in $k \in [0.044, 0.04475]$. After $k = 0.045$, the non-impact period-1 response emerges again as the control parameter k increases. To compare Figs. 7.4(a) and (b), the evolution of the calculated LEs is consistent with system's bifurcation, which is also demonstrated by the phase trajectories presented in Figs. 7.4(c)-(f).

8. Conclusions

This paper studies a numerical method for calculating the LEs of time-delayed piecewise-smooth systems by using a soft impacting system under the delayed feedback control with a particular focus on its near-grazing dynamics.

The main tasks were to build an effective variational equation and obtain the Jacobian matrix for the delayed impacting system. As the delayed impacting system is infinite dimensional, it was approximated by finite dimensional systems, which were linearised by the modified Euler integration method at each time step. Then the system was discretised by constructing a Poincaré map, and perturbation was introduced to obtain its variational equation. Then the Jacobian matrix of the map was obtained by combining all the approximated systems linearised from the variational equation at each time step in one period of external excitation. In order to increase the convergence rate and improve computational accuracy, a grazing estimation algorithm was studied. The convergence rate of eigenvalues of the Jacobian matrix was studied by using the spectral theory of the evolutionary operator. In particular, the delayed impacting system was described as an evolutionary operator whose convergence rate was the same as the relevant nonzero eigenvalues of the Jacobian matrix, therefore guaranteeing the reliability of the proposed numerical method.

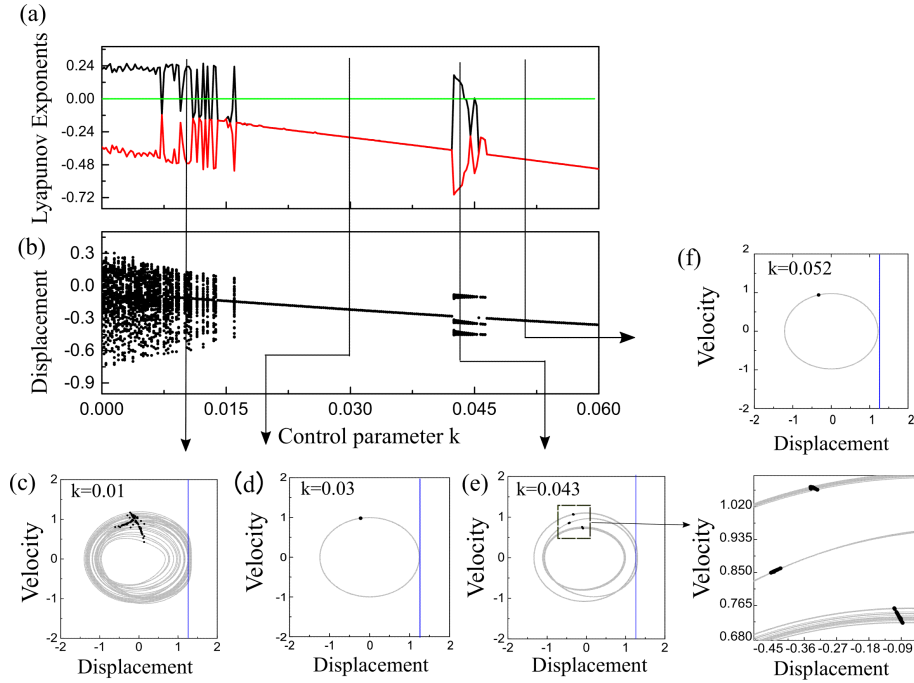


Figure 7.4: (a) LEs and (b) displacement of the impacting system under the delayed feedback controller as functions of the control parameter k . Black, red and green lines denote the two largest LEs and the zero line, respectively. Phase trajectories of the system calculated for (c) $k = 0.01$, (d) $k = 0.03$, (e) $k = 0.043$ and (f) $k = 0.052$ are shown. Black dots represent the Poincaré sections, and blue lines indicate the nonsmooth boundary.

Our numerical studies considered two scenarios of delay time in the system, a larger ($\tau_d \geq T$) and a smaller ($0 < \tau_d < T$) delay than the period of excitation. Both cases showed that the calculated LEs were consistent with the bifurcation of the system, and the grazing estimation algorithm had improved accuracy for simulating nonsmooth dynamical systems.

Acknowledgements

This work has been supported by EPSRC under Grant No. EP/P023983/1. Mr Zhi Zhang would like to acknowledge the financial support from the University of Exeter for his Exeter International Excellence Scholarship.

Compliance with ethical standards

Conflict of interest

The authors declare that they have no conflict of interest concerning the publication of this manuscript.

Data accessibility

The datasets generated and analysed during the current study are available from the corresponding author on reasonable request.

References

- [1] M. di Bernardo, C. Budd, A. R. Champneys, and P. Kowalczyk, *Piecewise-smooth dynamical systems: theory and applications*. Springer Science & Business Media, 2008.
- [2] J. Thompson and R. Ghaffari, “Chaos after period-doubling bifurcations in the resonance of an impact oscillator,” *Physics Letters A*, vol. 91, no. 1, pp. 5–8, 1982.
- [3] A. Muszynska and P. Goldman, “Chaotic responses of unbalanced rotor/bearing/stator systems with looseness or rubs,” *Chaos, Solitons & Fractals*, vol. 5, no. 9, pp. 1683–1704, 1995.
- [4] S. Yin, J. Ji, and G. Wen, “Complex near-grazing dynamics in impact oscillators,” *International Journal of Mechanical Sciences*, vol. 156, pp. 106–122, 2019.
- [5] J. Ing, E. Pavlovskaja, M. Wiercigroch, and S. Banerjee, “Bifurcation analysis of an impact oscillator with a one-sided elastic constraint near grazing,” *Physica D: Nonlinear Phenomena*, vol. 239, no. 6, pp. 312–321, 2010.
- [6] M. R. Jeffrey, A. Champneys, M. di Bernardo, and S. Shaw, “Catastrophic sliding bifurcations and onset of oscillations in a superconducting resonator,” *Physical Review E*, vol. 81, no. 1, p. 016213, 2010.
- [7] J. Ing, E. Pavlovskaja, M. Wiercigroch, and S. Banerjee, “Experimental study of impact oscillator with one-sided elastic constraint,” *Phil. Trans. R. Soc. A.*, vol. 366, no. 1866, pp. 679–705, 2007.
- [8] A. B. Nordmark, “Universal limit mapping in grazing bifurcations,” *Physical Review E*, vol. 55, no. 1, p. 266, 1997.
- [9] A. B. Nordmark, “Non-periodic motion caused by grazing incidence in an impact oscillator,” *Journal of Sound and Vibration*, vol. 145, no. 2, pp. 279–297, 1991.
- [10] G. Stépán and T. Insperger, “Stability of time-periodic and delayed systems—a route to act-and-wait control,” *Annual Reviews in Control*, vol. 30, no. 2, pp. 159–168, 2006.
- [11] S. Beregi, D. Takacs, and G. Stepan, “Bifurcation analysis of wheel shimmy with non-smooth effects and time delay in the tyre–ground contact,” *Nonlinear Dynamics*, pp. 1–18, 2019.
- [12] T. Zhang, X. Meng, and Y. Song, “The dynamics of a high-dimensional delayed pest management model with impulsive pesticide input and harvesting prey at different fixed moments,” *Nonlinear Dynamics*, vol. 64, no. 1-2, pp. 1–12, 2011.
- [13] A. R. Carvalho and C. M. Pinto, “New developments on aids-related cancers: The role of the delay and treatment options,” *Mathematical Methods in the Applied Sciences*, vol. 41, no. 18, pp. 8915–8928, 2018.
- [14] Y. Yan, J. Xu, and M. Wiercigroch, “Basins of attraction of the bistable region of time-delayed cutting dynamics,” *Physical Review E*, vol. 96, no. 3, p. 032205, 2017.
- [15] T. S. Parker and L. Chua, *Practical numerical algorithms for chaotic systems*. Springer Science & Business Media, 2012.

- [16] G. Benettin, L. Galgani, A. Giorgilli, and J.-M. Strelcyn, “Lyapunov characteristic exponents for smooth dynamical systems and for hamiltonian systems; a method for computing all of them. part 1: theory,” *Meccanica*, vol. 15, no. 1, pp. 9–20, 1980.
- [17] A. Wolf, J. B. Swift, H. L. Swinney, and J. A. Vastano, “Determining Lyapunov exponents from a time series,” *Physica D: Nonlinear Phenomena*, vol. 16, no. 3, pp. 285–317, 1985.
- [18] L. Dieci, R. D. Russell, and E. S. Van Vleck, “On the computation of Lyapunov exponents for continuous dynamical systems,” *SIAM Journal on Numerical Analysis*, vol. 34, no. 1, pp. 402–423, 1997.
- [19] A. Stefanski, “Estimation of the largest Lyapunov exponent in systems with impacts,” *Chaos, Solitons & Fractals*, vol. 11, no. 15, pp. 2443–2451, 2000.
- [20] P. C. Müller, “Calculation of Lyapunov exponents for dynamic systems with discontinuities,” *Chaos, Solitons & Fractals*, vol. 5, no. 9, pp. 1671–1681, 1995.
- [21] C. Dellago, H. A. Posch, and W. G. Hoover, “Lyapunov instability in a system of hard disks in equilibrium and nonequilibrium steady states,” *Physical Review E*, vol. 53, no. 2, p. 1485, 1996.
- [22] L. Jin, Q. Lu, and E. Twizell, “A method for calculating the spectrum of Lyapunov exponents by local maps in non-smooth impact-vibrating systems,” *Journal of Sound and Vibration*, vol. 298, no. 4-5, pp. 1019–1033, 2006.
- [23] H. Lamba and C. Budd, “Scaling of Lyapunov exponents at nonsmooth bifurcations,” *Physical Review E*, vol. 50, no. 1, p. 84, 1994.
- [24] J. D. Farmer, “Chaotic attractors of an infinite-dimensional dynamical system,” *Physica D: Nonlinear Phenomena*, vol. 4, no. 3, pp. 366–393, 1982.
- [25] J. Páez Chávez, Z. Zhang, and Y. Liu, “A numerical approach for the bifurcation analysis of nonsmooth delay equations,” *Communications in Nonlinear Science and Numerical Simulation*, vol. 83, p. 105095, 2020.
- [26] I. M. Repin, “On the approximate replacement of systems with lag by ordinary dynamical systems,” *Journal of Applied Mathematics and Mechanics*, vol. 29, no. 2, pp. 254–264, 1965.
- [27] I. Györi and J. Turi, “Uniform approximation of a nonlinear delay equation on infinite intervals,” *Nonlinear Analysis: Theory, Methods & Applications*, vol. 17, no. 1, pp. 21–29, 1991.
- [28] D. Breda, “Solution operator approximations for characteristic roots of delay differential equations,” *Applied Numerical Mathematics*, vol. 56, no. 3-4, pp. 305–317, 2006.
- [29] D. Breda, S. Maset, and R. Vermiglio, “Pseudospectral differencing methods for characteristic roots of delay differential equations,” *SIAM Journal on Scientific Computing*, vol. 27, no. 2, pp. 482–495, 2005.
- [30] D. Breda, S. Maset, and R. Vermiglio, “Approximation of eigenvalues of evolution operators for linear retarded functional differential equations,” *SIAM Journal on Numerical Analysis*, vol. 50, no. 3, pp. 1456–1483, 2012.
- [31] F. Chatelin, *Spectral approximation of linear operators*. SIAM, 2011.

- [32] Y. Liu and J. Páez Chávez, “Controlling coexisting attractors of an impacting system via linear augmentation,” *Physica D: Nonlinear Phenomena*, vol. 348, pp. 1–11, 2017.
- [33] K. Pyragas, “Continuous control of chaos by self-controlling feedback,” *Physics Letters A*, vol. 170, no. 6, pp. 421–428, 1992.
- [34] N. Krasovskii, “On the analytic construction of an optimal control in a system with time lags,” *Journal of Applied Mathematics and Mechanics*, vol. 26, no. 1, pp. 50–67, 1962.
- [35] H. Banks, “Approximation of nonlinear functional differential equation control systems,” *Journal of Optimization Theory and Applications*, vol. 29, no. 3, pp. 383–408, 1979.
- [36] J. Stoer and R. Bulirsch, *Introduction to numerical analysis*. Springer Science & Business Media, 2013.
- [37] H. Jiang and M. Wiercigroch, “Geometrical insight into non-smooth bifurcations of a soft impact oscillator,” *IMA Journal of Applied Mathematics*, vol. 81, no. 4, pp. 662–678, 2016.
- [38] F. Chatelin, “Convergence of approximation methods to compute eigenelements of linear operations,” *SIAM Journal on Numerical Analysis*, vol. 10, no. 5, pp. 939–948, 1973.
- [39] A. Varma and T. Mills, “On the summability of lagrange interpolation,” *Journal of Approximation Theory*, vol. 9, no. 4, pp. 349–356, 1973.